Cell. Mol. Biol. (ISSN: 1165-158X)

Journal Homepage: www.cellmolbiol.org

Cellular and Molecular Biology

Original Article

LncRNA MEG3 overexpression modulates proliferation without inducing apoptosis in rat cardiomyoblast h9c2 cells: a transcriptomic approach

Zhi Xing, Shajidan Abudureyimu, Palida Abulaiti, Yu Wang, Hui Li, Maolin Lyu, Ying Gao*

Department of Comprehensive Internal Medicine, The First Affiliated Hospital of Xinjiang Medical University, 830011 Urumqi, Xinjiang, China

Article Info

Article history:

Received: May 21, 2025
Accepted: June 25, 2025
Published: September 30, 2025

Use your device to scan and read the article online

Abstract

Long non-coding RNAs (lncRNAs) have been implicated in various biological processes including cell proliferation and apoptosis. However, the role of lncRNA-MEG3 in rat cardiomyoblast H9C2 cells remains unclear. In this study, H9C2 cells were genetically modified to overexpress lncRNA MEG3. The proliferation of these cells was evaluated using the Cell Counting Kit-8 (CCK-8) assay and direct imaging techniques. Apoptosis was assessed through flow cytometry, employing Annexin V and propidium iodide (PI) staining. Quantitative PCR was utilized to confirm the overexpression of lncRNA MEG3. Further, differential expression and alternative splicing analyses were conducted using comprehensive transcriptome sequencing. The overexpression of lncRNA MEG3 in H9C2 cells led to a significant reduction in cell proliferation, as evidenced by lower absorbance readings in the CCK-8 assay and reduced cell confluency in imaging analyses. However, flow cytometric analysis revealed no substantial differences in apoptosis between the lncRNA MEG3 overexpressing group and the control. Transcriptomic analyses demonstrated significant changes in gene expression and alternative splicing patterns, highlighting the intricate role of lncRNA MEG3 in cellular regulatory mechanisms. In conclusion, lncRNA MEG3 overexpression in rat cardiomyoblast H9C2 cells significantly inhibits cellular proliferation without markedly inducing apoptosis, suggesting a specific regulatory role in cellular growth processes. The transcriptomic alterations observed underscore the potential of lncRNA MEG3 as a key player in the molecular dynamics of cardiomyoblasts.

Keywords: lncRNA MEG3, Cardiomyoblasts, H9C2 cells, Proliferation, Apoptosis, Transcriptomic analysis, Alternative splicing.

1. Introduction

Cardiovascular diseases (CVDs) are the main global cause of death, claiming about 17.9 million lives annually. Over 80% of these deaths result from heart attacks and strokes, and one-third occur in individuals younger than 70 years [1-3]. CVDs costs are continuing to rise, posing significant challenges to public health systems. Heart failure, a common outcome of various CVDs, is characterized by the heart's inability to pump sufficient blood to meet the body's needs [4]. The financial burden of cardiovascular diseases (CVDs) is growing, presenting major challenges to healthcare systems. Heart failure, often a consequence of CVDs, occurs when the heart cannot pump enough blood to satisfy the body's demands [5]. The molecular mechanisms behind heart failure are complex and not completely understood, which hampers the creation of more effective targeted treatments.

Recently, long non-coding RNAs (lncRNAs), which are RNA transcripts over 200 nucleotides long and do not code for proteins, have been recognized for their regulatory roles in gene expression and their involvement in the development of diseases, including cardiovascular diseases (CVDs) [6]. They are involved in diverse cellular processes such as chromatin remodeling, transcriptional control, and post-transcriptional processing [7]. LncRNAs can be transcribed by RNA polymerase I, II, and III, as well as from processed introns. They include intergenic lincRNAs, intronic ncRNAs, and sense and antisense lncRNAs, each with different genomic positions in relation to genes and exons [8]. Despite their lack of protein-coding potential, lncRNAs exhibit cellular functions and are reported to be involved in ceRNA regulation, transcriptional regulation, and epigenetic regulation [9]. LncRNAs are a significant and functionally diverse class of RNA molecules, despite being initially regarded as "dark matter" in the genome [10]. Among these, lncRNA MEG3 has been identified as a key regulator in several biological contexts, including tumorigenesis and developmental processes [11].

Our study bridges the gap between the pathological significance of heart failure and the regulatory mechanisms of lncRNA MEG3. We hypothesize that lncRNA MEG3 plays a pivotal role in modulating cellular processes in cardiomyoblasts, which could have implications for unders-

* Corresponding author.
E-mail address: 19397885802@163.com (Y. Gao).
Doi: http://dx.doi.org/10.14715/cmb/2025.71.9.2

tanding heart failure's molecular basis. To investigate this, we focus on the effects of lncRNA MEG3 overexpression in rat cardiomyoblast H9C2 cells, examining its impact on cell proliferation and apoptosis. Additionally, we undertake a comprehensive transcriptomic analysis to unravel the broader implications of MEG3 modulation in cardiac cell biology. This research aims to provide valuable insights into the potential of lncRNA MEG3 as a therapeutic target in heart failure and contribute to the broader understanding of lncRNA functions in cardiac diseases.

2. Materials and Methods

2.1. Cell culture and transfection

The rat cardiomyoblast H9C2 cell line, derived from embryonic BD1X rat heart tissue, was utilized for this study. Cells were cultured in Dulbecco's Modified Eagle Medium (DMEM) supplemented with 10% fetal bovine serum (FBS), 100 units/mL penicillin, and 100 µg/mL streptomycin. The culture environment was maintained at 37°C in a humidified atmosphere containing 5% CO_2. Cells were passaged upon reaching approximately 80% confluency using 0.25% trypsin-EDTA solution.

For the overexpression of lncRNA MEG3, H9C2 cells were transfected with either a plasmid vector carrying the MEG3 sequence or a control vector. Prior to transfection, cells were seeded in 6-well plates and allowed to reach 70-80% confluency. Transfection was performed using Lipofectamine 3000 reagent according to the manufacturer's instructions. Briefly, the plasmid DNA and Lipofectamine 3000 were diluted separately in Opti-MEM reduced serum medium and then combined to form the DNA-lipid complex. The cells were incubated with the transfection mixture for 6 hours, after which the medium was replaced with fresh DMEM containing 10% FBS. The efficiency of transfection was evaluated 48 hours post-transfection through quantitative PCR analysis of MEG3 expression.

2.2. Confirmation of lncRNA MEG3 overexpression

Total RNA was extracted from transfected H9C2 cells using the TRIzol reagent, following the manufacturer's protocol. The quality and concentration of RNA were determined using a NanoDrop spectrophotometer. cDNA was synthesized from 1 µg of total RNA using a reverse transcription kit according to the manufacturer's instructions.

qPCR was performed to quantify lncRNA MEG3 expression levels using SYBR Green PCR Master Mix.

Specific primer sequences for lncRNA MEG3 were as follows:
Forward Primer: 5'-AGAAGGCTGGGGCTCATTTG-3',
Reverse Primer: 5'-AGGGGCCATCCACAGTCTTC-3'.
GAPDH was used as an internal control, with the following primer sequences:
Forward Primer: 5'-TGCACCACCAACTGCTTAGC-3',
Reverse Primer: 5'-GGCATGGACTGTGGTCATGAG-3'.

The qPCR reactions were set up in a total volume of 20 µL, including 10 µL of SYBR Green PCR Master Mix, 1 µL of each primer (10 µM), 2 µL of cDNA template, and 6 µL of nuclease-free water. The amplification conditions were as follows: initial denaturation at 95°C for 10 minutes, followed by 40 cycles of denaturation at 95°C for 15 seconds, annealing at 60°C for 1 minute, and extension at 72°C for 30 seconds. The specificity of the PCR products was confirmed by melting curve analysis. The relative expression levels of lncRNA MEG3 were calculated using the 2^-ΔΔCt method. Data were normalized to the expression levels of GAPDH. Statistical analysis was performed to compare the expression levels of lncRNA MEG3 between the transfected and control groups.

2.3. Proliferation assay

2.3.1. Cell counting Kit-8 (CCK-8) assay

The CCK-8 assay was employed to assess the proliferation of H9C2 cells post-transfection. Following transfection, cells were seeded in 96-well plates at a density of 5,000 cells per well and incubated for specific time intervals (0, 24, 48, and 72 hours). At each time point, 10 µL of CCK-8 solution was added to each well, followed by incubation for 2 hours at 37°C. The absorbance at 450 nm was measured using a microplate reader, indicating cell viability as a proxy for cell proliferation. The assay was conducted in triplicate for each time point to ensure the reliability of the results.

2.3.2. Direct imaging

In parallel with the CCK-8 assay, direct imaging of the cells was performed to provide a qualitative assessment of cell proliferation. Cells were seeded in 6-well plates and monitored at the same time intervals as the CCK-8 assay. Images were captured using an inverted microscope at 10x magnification to observe changes in cell confluency and morphology. The number of cells in representative fields was counted to provide a visual assessment of cell proliferation over time.

For the CCK-8 assay, the absorbance data were plotted to generate growth curves for each group. Statistical analysis was performed to compare the proliferation rates between the lncRNA MEG3 overexpressing cells and the control group. The direct imaging data were used to qualitatively corroborate the findings from the CCK-8 assay. ImageJ software was utilized for the quantification of cell numbers from the images, when applicable.

2.4. Apoptosis analysis

At 48 hours post-transfection, H9C2 cells overexpressing lncRNA MEG3 and control cells were harvested for apoptosis analysis. Cells were detached using trypsin-EDTA, neutralized with complete medium, and then collected by centrifugation. The cell pellet was washed twice with cold phosphate-buffered saline (PBS) and resuspended in 1X binding buffer at a concentration of 1 x 10^6 cells/mL.

The cell suspension was stained using the Annexin V-FITC/PI apoptosis detection kit following the manufacturer's instructions. Briefly, 100 µL of the cell suspension was transferred to a new tube, and 5 µL of Annexin V-FITC and 5 µL of PI were added. The cells were gently vortexed and incubated for 15 minutes at room temperature in the dark. After incubation, 400 µL of 1X binding buffer was added to each tube. Stained cells were analyzed using a flow cytometer equipped with a 488 nm laser for excitation. FITC and PI fluorescence emissions were detected in the FL1 (green) and FL2 (red) channels, respectively. A minimum of 10,000 events per sample were recorded. The flow cytometer was calibrated using unstained, single-stained, and fluorescence-minus-one (FMO) controls to set the appropriate gates and compensation. FlowJo software was used to analyze the flow cytometry data. Cells were gated on forward and side scatter to exclude debris. Dou-

blets were excluded using forward scatter height versus forward scatter area gating. Apoptotic cells were quantified as follows: early apoptotic cells (Annexin V positive, PI negative) and late apoptotic/necrotic cells (Annexin V positive, PI positive). The percentage of apoptotic cells in each sample was calculated and compared between the lncRNA MEG3 overexpressing group and the control group. Statistical analyses were performed to determine significant differences in apoptosis rates.

2.5. Transcriptome sequencing and analysis

At 48 hours post-transfection, total RNA was isolated from the lncRNA MEG3 overexpressed and control H9C2 cells using the TRIzol reagent. RNA integrity and quality were assessed using the Agilent 2100 Bioanalyzer. RNA samples with an integrity number (RIN) >7 were used for library preparation. Sequencing libraries were prepared using the TruSeq RNA Library Prep Kit, following the manufacturer's protocol, which included steps for poly-A mRNA isolation, fragmentation, cDNA synthesis, adapter ligation, and amplification. The prepared libraries were sequenced on the Illumina NovaSeq 6000 platform. Paired-end sequencing was performed with a read length of 150 base pairs (bp). Each sample was sequenced to a depth of approximately 40 million reads to ensure adequate coverage and depth for reliable differential expression analysis.

Raw sequencing data were first subjected to quality control checks using FastQC. Reads were trimmed for adapter sequences and low-quality bases using Trimmomatic. Cleaned reads were then aligned to the rat reference genome (Rattus norvegicus) using the STAR RNA-seq aligner. Differential gene expression analysis was conducted using DESeq2, with genes identified as differentially expressed based on a fold change threshold of ≥ 1.5 or ≤ 0.666 and an adjusted P-value < 0.05. Alternative splicing analysis was performed using rMATS, which identifies and quantifies differential alternative splicing events between the two groups. Gene Ontology (GO) enrichment and Kyoto Encyclopedia of Genes and Genomes (KEGG) pathway analyses were conducted on differentially expressed genes and alternatively spliced genes using DAVID and KEGG Orthology-Based Annotation System (KOBAS).

2.6. Statistical analysis

In our study, we employed the online program DAVID Bioinformatics Resources 6.7 (https://david.ncifcrf.gov/) for plotting the GO figure. To identify statistically significant pathways and diseases associated with DEGs, we utilized KOBAS 3.0 (http://bioinfo.org/kobas). For clustering analysis, the values were adjusted by mean centering and normalizing the genes, and then clustered by a city-block distance–based complete linkage hierarchical method. Heatmaps to visualize these results were generated using Gene Cluster 3.0. In terms of data presentation, parameters that were normally distributed are expressed as mean ± SEM. For parameters that were not normally distributed, data are presented as the median along with the 25th to 75th percentile range. To test differences between groups for variables with normal distribution, we employed the t-test or analysis of variance (ANOVA).

All statistical analyses were performed using GraphPad Prism 8 (GraphPad Software, San Diego, CA). A P-value of less than 0.05 was considered to indicate statistical significance.

3. Results

3.1. Differential expression of lncRNA MEG3 in heart failure: Insights from GSE147236 dataset analysis

Our differential expression analysis of the GSE147236 dataset, involving healthy individuals and heart failure (HF) patients, revealed a distinct profile of differentially expressed long non-coding RNAs (lncRNAs). A principal component analysis (PCA) was executed to evaluate the variations in lncRNA expression patterns between the HF patients and healthy controls. The PCA plot (Fig. 1A) illustrates a pronounced separation between the two groups along the first principal component (Dim1), which explains 20.9% of the total variance, and the second principal component (Dim2), accounting for 12.7%. The HF samples formed a distinct cluster, signifying a specific lncRNA expression profile associated with the heart failure state. Furthermore, a volcano plot (Fig. 1B) was constructed to provide a visual representation of the differentially expressed lncRNAs between the HF and healthy control groups. The plot accentuates upregulated lncRNAs in

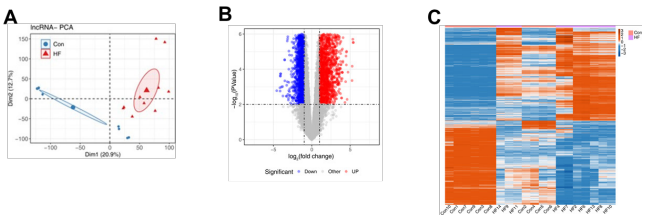

Fig. 1. Differential expression analysis of lncRNA in heart failure. (A) Principal Component Analysis (PCA) Plot: The PCA plot demonstrates the separation between control (Con) and heart failure (HF) samples based on the expression profiles of long non-coding RNAs (lncRNAs). The first principal component (Dim1) accounts for 20.9% of the variance, and the second principal component (Dim2) accounts for 12.7%, indicating distinct lncRNA expression patterns between the two groups. (B) Volcano Plot: This plot visualizes the differential expression of lncRNAs between HF and control samples. Upregulated lncRNAs in the HF group are shown in red, and downregulated lncRNAs are in blue. The significance threshold is set at a fold change of ≥2 or ≤0.5 and a P-value < 0.01, with significant lncRNAs standing out above the threshold line. (C) Heatmap of lncRNA Expression: The heatmap displays the expression levels of lncRNAs across all samples, with each row representing an lncRNA and each column representing a sample. Expression levels are color-coded: red indicates upregulation, blue indicates downregulation. The clear distinction between the control and HF samples reflects the specific expression trends associated with heart failure.

Table 1. Summary of Differentially Expressed Genes (DEGs)

DEG group	Up regulated gene NO.	Down regulated gene NO.	Total
HF_vs_con	1824	1652	3476

The table summarizes the number of upregulated and downregulated genes identified in the HF group compared to controls. A total of 1824 genes were found to be upregulated, while 1652 were downregulated, amounting to 3476 DEGs in the HF vs. control comparison.

red and downregulated ones in blue, with the significant lncRNAs, including MEG3, indicated above the defined threshold line, which is set at a fold change of ≥2 or ≤0.5 and a P-value < 0.01. The expression patterns of the differentially expressed lncRNAs are summarized in a heatmap (Fig. 1C). This heatmap aligns each lncRNA (row) against the respective sample (column), with color gradations representing expression levels: red for upregulation and blue for downregulation. This heatmap is instrumental in highlighting the expression trends across the dataset and pinpointing lncRNAs like MEG3, which may play a pivotal role in the pathogenesis of heart failure.

3.2. Impact of lncRNA MEG3 overexpression on proliferation and apoptosis in rat cardiomyoblast H9C2 cells

To investigate the effects of lncRNA MEG3 on the proliferation and apoptosis of rat cardiomyoblast H9C2 cells, we engineered an overexpression cell line. The proliferation of these cells was assessed through two distinct methodologies: direct imaging and the Cell Counting Kit-8 (CCK-8) assay. Apoptosis was evaluated using flow cytometry with Annexin V and propidium iodide (PI) staining. The overexpression of lncRNA-MEG3 was confirmed through quantitative PCR analysis (Fig. 2A). Subsequent to the confirmation of overexpression, the proliferative capacity of the H9C2 cells was quantitatively assessed. Direct imaging of the cells provided a qualitative visual confirmation that lncRNA-MEG3 overexpression resulted in a noticeable reduction in cell confluency over time, suggesting an inhibitory effect on cell growth (Fig. 2B). The CCK-8 assay quantified this observation; the absorbance readings, indicative of viable cell numbers, were significantly lower in the lncRNA-MEG3 overexpressing cells compared to the control group ($p < 0.05$) (Fig. 2C-G). This reduction in proliferation was evident across multiple time points, reinforcing the inhibitory effect of lncRNA-MEG3 overexpression on cardiomyoblast cell growth.

Flow cytometric analysis, utilizing Annexin V and PI staining, was employed to distinguish apoptotic cells in the H9C2 cell population. The results showed no significant difference in the percentage of early apoptotic (Annexin V positive, PI negative) and late apoptotic (Annexin V positive, PI positive) cells between the lncRNA-MEG3 overexpressing group and the control group (Fig. 2H). These findings indicate that while lncRNA-MEG3 overexpression suppresses the proliferation of H9C2 cells, it does not exert a significant impact on the induction of apoptosis under the conditions tested. These findings suggest a specific role of lncRNA-MEG3 in modulating cellular growth processes in cardiac-derived cells, which could have implications for understanding the molecular mechanisms underlying cardiac pathologies and diseases.

3.3. Differential expression analysis in H9C2 cardiomyoblasts following lncRNA MEG3 transfection

To elucidate the mechanistic roles of lncRNA MEG3, H9C2 cardiomyoblasts were transfected with either lncRNA MEG3 or a control vector across three biological replicates. Comprehensive transcriptome sequencing was conducted, followed by differential gene expression analysis and differential alternative splicing analysis. Correlation analysis between the samples revealed a high degree of concordance in gene expression profiles, particularly

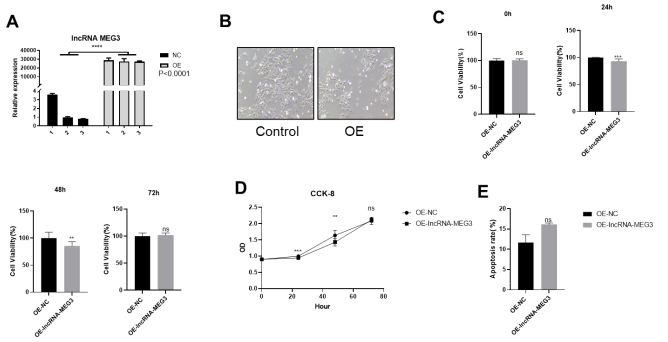

Fig. 2. Effects of lncRNA MEG3 Overexpression on Cell Proliferation and Apoptosis in H9C2 Cells. (A) lncRNA MEG3 Expression Analysis: Quantitative PCR results showing lncRNA MEG3 expression levels in H9C2 cells. Overexpression (OE) of lncRNA MEG3 is confirmed with significantly higher expression levels compared to the negative control (NC), indicated by the bar graph (****P<0.0001). (B) Representative Cell Morphology: Microscopic images depict the morphology of H9C2 cells in the control group and the lncRNA MEG3 overexpressed group, illustrating the physical differences in confluency and cell structure. (C) Cell Viability Assay: Bar graphs display the viability of H9C2 cells after overexpression of lncRNA MEG3, with a noticeable decrease in cell viability in the OE group at 24h (***P<0.001). (D) CCK-8 Proliferation Assay: A line graph illustrates the results of the CCK-8 assay over time (0, 24, 48, and 72 hours). There is a significant reduction in cell proliferation in the lncRNA MEG3 overexpressed group compared to the control at 48 hours (**P<0.01) and 72 hours (ns - not significant). (E) Apoptosis Analysis: Bar graphs show the percentage of apoptotic cells in both the control and lncRNA MEG3 overexpressed H9C2 cells, indicating no significant difference in apoptosis rates between the two groups (ns - not significant).

within the biological replicates, suggesting that the transfection process was consistent and reliable (Fig. 3A). Clustering analysis based on these correlations confirmed the close relationship between samples within the same experimental group, indicating a specific gene expression signature associated with lncRNA MEG3 overexpression. Utilizing DESeq2 for the identification of differentially expressed genes (DEGs), our analysis accounted for library depth and normalized for transcript length through FPKM calculation. DEGs were pinpointed using a fold change threshold of ≥ 1.5 or ≤ 0.666 and a P-value of < 0.05. The volcano plot (Fig. 3B) stratified the genes into significantly upregulated, downregulated, and those without significant changes. This analysis revealed that transfection with lncRNA MEG3 led to 29 genes being significantly upregulated and 53 genes significantly downregulated, thereby highlighting the specific regulatory impact of MEG3 on the cardiomyoblast transcriptome. A heatmap was constructed for all significant DEGs, revealing distinctive patterns of gene expression (Fig. 3C). The heatmap underscored the expression modulations in H9C2 cells due to lncRNA MEG3 overexpression, with particular gene clusters exhibiting heightened expression changes. Gene Ontology (GO) enrichment analysis of the DEGs revealed associations with diverse biological processes, molecular functions, and cellular components, shedding light on the roles of lncRNA MEG3 in cellular dynamics. Notably, the analysis identified significant enrichment in terms such as plasma membrane and extracellular exosomes (Fig. 3D),

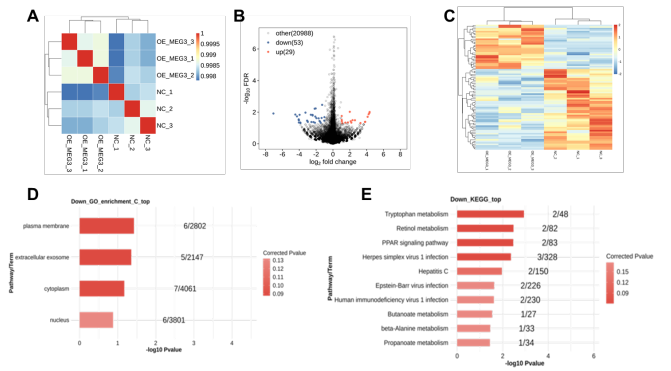

Fig. 3. Transcriptomic changes induced by lncRNA MEG3 overexpression. (A) Sample Correlation Heatmap: The heatmap illustrates the correlation between different samples. Each square represents the correlation coefficient between the samples labeled on the x and y axes. Overexpressed MEG3 (OE_MEG3) samples show high correlation with each other, as do the negative control (NC) samples, indicating consistency within groups. (B) Volcano Plot: This plot displays the differential gene expression upon MEG3 overexpression. Each dot represents a gene; red dots indicate significantly upregulated genes, blue dots indicate significantly downregulated genes, and gray dots represent genes without significant changes. The x-axis represents the log2 fold change, while the y-axis shows the negative log10 of the false discovery rate (FDR). Points further to the right or left indicate greater fold changes, and points higher on the plot indicate lower FDR values. (C) Gene Expression Heatmap: The heatmap shows gene expression levels across all samples, with rows representing individual genes and columns representing different samples. Red indicates higher expression levels, and blue indicates lower levels. The clustering on the top indicates similar expression patterns among samples. (D) GO Enrichment Analysis of Downregulated Genes: The bar graph represents GO categories that are significantly enriched among downregulated genes. Each bar's length represents the negative log10 P-value of the enrichment, with categories listed on the y-axis and the number of genes/out of total in that category on the bars. (E) KEGG Pathway Enrichment Analysis of Downregulated Genes: This bar graph depicts the top KEGG pathways enriched among downregulated genes. The pathways are listed on the y-axis, with bars representing the negative log10 P-value of the enrichment. The number of affected genes/total genes in the pathway is shown on each bar, with a lower P-value indicating more significant enrichment.

which underscores the potential involvement of MEG3 in cellular communication and signaling modalities. Furthermore, the Kyoto Encyclopedia of Genes and Genomes (KEGG) pathway enrichment analysis delineated several pathways that were notably represented among the DEGs, including tryptophan metabolism and retinol metabolism (Fig. 3E). In summary, the differential expression and enrichment analyses post-lncRNA MEG3 transfection have revealed alterations in gene expression and implicated pathways that could contribute to the understanding of the biological functions and mechanisms of action of lncRNA MEG3 in cardiomyoblasts.

3.4. Differential expression and alternative splicing analysis of lncRNAs

In our study, we performed a GO enrichment analysis on differentially expressed lncRNAs (DElncRNAs) and their co-expressed DEGs. The aim was to elucidate the functional roles of these lncRNAs in various molecular functions, biological processes, and cellular components. By aligning DElncRNA targets to a range of GO terms and applying a hypergeometric distribution test against the backdrop of the whole genome's GO annotations, we uncovered significant enrichments in specific GO terms. Notably, among the top 10 enriched GO terms presented in Figure 10, 'plasma membrane' and 'extracellular exosomes' were highlighted (Fig. 4A), indicating these areas as key sites of DElncRNA activity. In parallel, a KEGG pathway enrichment analysis was undertaken to explore the potential involvement of DElncRNAs in diverse biological pathways and systems. This involved mapping DElncRNAs and their co-expressed DEGs to KEGG pathways and assessing the enrichment using a hypergeometric test. Our analysis identified several pathways significantly enriched with these targets. The most prominent pathways, determined by their corrected P-values, include 'Gap junction' and 'Parathyroid hormone synthesis, secretion, and action.' These findings provide a deeper insight into the complex networks and pathways potentially regulated by these lncRNAs, underscoring their importance in cellular communication and hormonal regulation mechanisms.

Furthermore, our analysis extended to include differential alternative splicing (AS) events. The AS analysis,

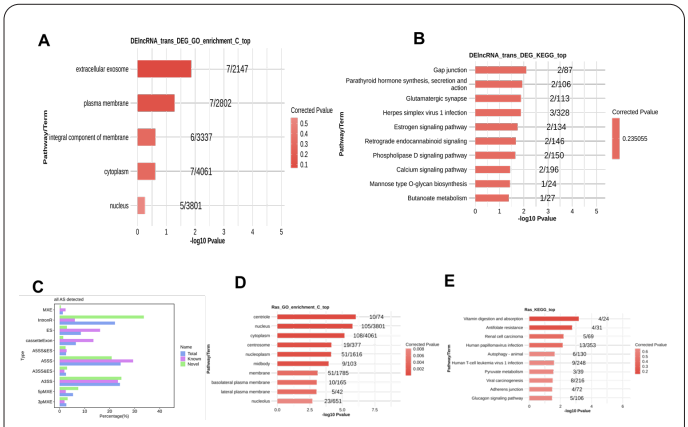

Fig. 4. Comprehensive analysis of lncRNA-associated transcriptomic changes and functional enrichment. (A) GO Enrichment Analysis for DEGs: The bar chart illustrates the cellular components enriched in DEGs associated with differentially expressed lncRNAs (DElncRNAs). The x-axis represents the negative log10 P-value, indicating the statistical significance of enrichment, with cellular components such as the extracellular exosome, plasma membrane, and cytoplasm highlighted. (B) KEGG Pathway Enrichment Analysis for DEGs: This bar chart displays the top enriched pathways for DEGs related to DElncRNAs, with the negative log10 P-value on the x-axis. Pathways like gap junction, parathyroid hormone synthesis, secretion and action, and glutamatergic synapse are among the significantly enriched. (C) Alternative Splicing Events: The histogram shows the distribution of different types of alternative splicing events detected in the analysis. The x-axis indicates the percentage of events, categorized into types such as exon skipping (ES) and mutually exclusive exons (MXE). (D) GO Enrichment Analysis for Target Genes of DElncRNAs: The bar chart shows the cellular components with significant enrichment in target genes of DElncRNAs. The x-axis shows the negative log10 P-value, with components such as the nucleus, centrosome, and plasma membrane being significantly enriched. (E) KEGG Pathway Enrichment Analysis for Target Genes of DElncRNAs: This bar chart presents the top enriched KEGG pathways in the target genes of DElncRNAs, with the negative log10 P-value on the x-axis. Notable pathways include vitamin digestion and absorption, antifolate resistance, and renal cell carcinoma.

visualized in Fig. 4C (All_AS_detected_Bar), provided insights into the complex regulatory mechanisms at the RNA level. We conducted a GO enrichment analysis for genes undergoing differential AS, aiming to uncover the biological significance of these splicing events. The top 10 enriched GO terms for these genes, as shown in Fig. 4D, underscore the importance of AS in critical cellular processes, including 'centriole' and 'nucleus', highlighting key areas of AS activity. Similarly, KEGG pathway enrichment analysis was performed for these genes, revealing significant enrichment in specific pathways (Fig. 4E), notably 'Vitamin digestion and absorption' and 'Antifolate resistance'. These findings illuminate the involvement of differential AS in distinct biological pathways, suggesting a broader impact on nutrient metabolism and cellular responses to external agents.

4. Discussion

In this study, we investigated the role of long non-coding RNA (lncRNA) MEG3 in the regulation of cell proliferation and apoptosis in rat cardiomyoblast H9C2 cells. Our findings demonstrated that overexpression of lncRNA MEG3 in these cells significantly inhibited cell proliferation. Additionally, comprehensive transcriptome sequencing revealed significant changes in gene expression and alternative splicing patterns, suggesting a complex role of lncRNA MEG3 in cellular regulatory mechanisms. These findings underscore the potential of lncRNA MEG3 as a key player in the molecular dynamics of cardiomyoblasts and its specific regulatory role in cellular growth processes.

The observed reduction in proliferation of H9C2 cells with lncRNA MEG3 overexpression aligns with the growing evidence suggesting lncRNAs play a critical role in cardiac cell growth and function. Studies have indicated that deregulation of certain lncRNAs is associated with cardiac hypertrophy and heart failure. For example, the lncRNA Mhrt has been found to antagonize the function of Brg1, a chromatin-remodeling factor, which is activated by stress to trigger aberrant gene expression, leading to cardiac hypertrophy and failure [12]. Additionally, lncRNA AHIT has been shown to protect against cardiac hypertrophy through SUZ12 (Suppressor of Zeste 12 Protein Homolog) [13]. These findings suggest that lncRNAs play a significant role in the development of cardiac hypertrophy and heart failure, and they may serve as potential therapeutic targets.

The proliferation of cardiomyocytes in the context of heart disease is a double-edged sword. While it is necessary for cardiac repair and regeneration, uncontrolled proliferation can lead to pathological hypertrophy. Cardiomyocyte proliferation is regulated during heart development, growth, and homeostasis. It is essential for cardiac repair and regeneration, particularly in the neonatal stage, but in adults, the capacity for cardiomyocyte proliferation is limited, leading to pathological hypertrophy and heart failure [14-16]. The failure of adult cardiomyocytes to reproduce themselves to repair an injury results in the development of severe cardiac disease [17]. Additionally, uncontrolled proliferation of cardiomyocytes can lead to pathological hypertrophy, which is detrimental to heart function [18]. The inhibitory effect of MEG3 on cell proliferation might, therefore, represent a protective mechanism against hypertrophy. The heart is a highly energy-demanding organ, and excessive apoptosis of cardiomyocytes can lead to detrimental outcomes in heart disease. The absence of an apoptotic response to MEG3 overexpression may thus reflect a protective mechanism, allowing for the regulation of cell growth without triggering cell death, which is consistent with the findings of some studies emphasizing the protective roles of certain lncRNAs in cardiac cells [19].

4.1. Comparative analysis with previous studies

Our study's observation of transcriptomic alterations due to MEG3 overexpression in cardiomyoblasts adds to a growing body of research on this lncRNA in various cell types. For instance, in cancer biology, MEG3 has been shown to influence gene expression patterns significantly, often leading to the suppression of tumor growth and metastasis [20]. In neurological studies, MEG3 has been implicated in the regulation of neuronal death and neurodegenerative diseases [21]. Unlike these studies, where MEG3 overexpression can induce cell death, our study in cardiomyoblasts suggests a protective role against uncontrolled cell growth, hinting at a multifaceted role of MEG3 across different tissues. The diversity in the roles of MEG3 across different cell types and diseases underscores its complexity as a regulatory molecule. In the context of cardiac cells, MEG3 appears to function differently from its role in cancer or neuronal cells. This has important implications for therapeutic strategies targeting MEG3, as its effects may vary significantly depending on the target tissue or disease state.

4.2. Mechanistic insights and hypotheses

The observed transcriptomic changes in our study suggest that MEG3 may act as a molecular scaffold or guide, bringing together various protein complexes that influence gene expression and RNA processing. This hypothesis is supported by studies showing that lncRNAs can recruit chromatin-modifying enzymes to specific genomic regions, thereby affecting gene expression [22]. Regarding alternative splicing, MEG3 could interact with splicing factors or modulate the expression of these factors, thereby influencing splice site selection and exon inclusion in pre-mRNA. This aligns with research indicating that lncRNAs can modulate splicing either by direct interactions with the splicing machinery or by altering the expression of splicing factors [23]. One potential mechanism by which MEG3 influences cellular proliferation is through the modulation of cell cycle-related genes. Our transcriptomic analysis revealed changes in the expression of several genes involved in the cell cycle, suggesting that MEG3 may exert its effects by upregulating inhibitors or downregulating promoters of cell cycle progression. Another hypothesis is that MEG3 affects signaling pathways known to regulate cardiomyoblast proliferation. For instance, MEG3 could influence the activity of pathways such as the MAPK/ERK or PI3K/Akt pathways, both of which are crucial in controlling cell growth and proliferation in cardiac cells [24]. Additionally, MEG3 might regulate the expression of growth factors or their receptors in cardiomyoblasts, thereby indirectly influencing proliferative signaling. These hypotheses provide a foundation for future experimental investigations to elucidate the precise mechanisms by which MEG3 regulates cellular processes in cardiomyoblasts.

4.3. Clinical and therapeutic implications

Our findings that lncRNA MEG3 overexpression leads to reduced proliferation in cardiomyoblasts could have significant implications for understanding the pathogenesis of heart diseases. In the context of cardiac repair and regeneration, controlling cardiomyocyte proliferation is crucial. The ability of MEG3 to regulate this process might be harnessed to prevent pathological cardiac remodeling and hypertrophy, common features in various heart diseases, including heart failure and myocardial infarction [25]. Additionally, the role of MEG3 in modulating transcriptomic profiles suggests that it might be involved in fine-tuning the expression of genes critical for cardiac function and response to stress. This understanding could provide new insights into the molecular basis of heart diseases and potentially reveal novel biomarkers for early detection or prognosis. The therapeutic targeting of lncRNAs like MEG3 in heart disease presents a novel and promising avenue. However, this approach also poses significant challenges. Delivering lncRNA-based therapeutics to the heart specifically, and ensuring sustained and controlled expression, remains a major obstacle [26]. Potential strategies for targeting MEG3 could involve the use of small molecules, antisense oligonucleotides, or RNAi-based approaches to modulate its expression. The development of such targeted therapies would require a deeper understanding of MEG3's interactions and effects in the cardiac cellular environment. Another challenge is the specificity of lncRNA functions. Given that MEG3 has been implicated in various biological processes across different cell types, ensuring target specificity to avoid off-target effects is crucial. This necessitates the development of cardiac-specific delivery systems or targeting strategies. In summary, while the therapeutic targeting of MEG3 in heart disease holds promise, significant research and development are needed to address the challenges of specificity, delivery, and safety in clinical applications.

4.4. Limitations and future directions

4.4.1. Study limitations

A primary limitation of our study is the reliance on an in vitro model using rat cardiomyoblast H9C2 cells. While this model offers valuable insights, it cannot fully replicate the complexity of human heart tissues or the systemic interactions present in a living organism. Therefore, the results might not be entirely translatable to human physiology. The scope of our analysis was focused on the overexpression of MEG3 and its immediate effects on proliferation and apoptosis. We did not explore the downstream signaling pathways or the direct gene targets affected by MEG3, which limits the depth of our mechanistic understanding.

4.4.2. Future research directions

Future studies should aim to validate our findings in vivo, using animal models of heart disease. This will provide a more comprehensive understanding of MEG3's role in cardiac physiology and pathology. Investigating the direct targets and interacting partners of MEG3 in cardiomyocytes will be crucial to elucidate its molecular mechanisms. Techniques such as RNA immunoprecipitation followed by sequencing (RIP-Seq) could be employed to identify proteins interacting with MEG3. Further research is needed to explore the potential of MEG3 as a therapeutic target. This includes the development of targeted delivery systems and the evaluation of efficacy and safety in preclinical models.

4.5. Broader implications in molecular biology

Our study contributes to the expanding field of lncRNA research by highlighting the specific roles of MEG3 in cardiomyoblasts. It underscores the versatility and complexity of lncRNA functions across different cell types and physiological contexts.

The findings emphasize the significance of lncRNAs in cellular regulation, particularly in critical processes like cell proliferation and transcriptomic modulation. This reinforces the concept that lncRNAs are not mere byproducts of transcription but key regulatory elements in cellular biology. By demonstrating the specific effects of MEG3 in a cardiac cell line, our study adds to the growing understanding of how lncRNAs can influence cell fate and function. It provides a basis for further exploration into the therapeutic potential of modulating lncRNA activity in heart diseases. The study also highlights the need for comprehensive research into the diverse roles of lncRNAs in health and disease, paving the way for novel diagnostic and therapeutic approaches in molecular medicine.

Our study demonstrates that lncRNA MEG3 plays a crucial role in regulating proliferation in rat cardiomyoblast H9C2 cells, highlighting its potential significance in heart disease. The specific influence of MEG3 on cell growth, without affecting apoptosis, offers new insights into cardiac cellular regulation and points to its potential as a therapeutic target. These findings contribute to the broader understanding of lncRNA functions in cardiac health and disease, paving the way for future research in this field.

Acknowledgements

This work was supported by grants from the Natural Science Foundation of Xinjiang Uygur Autonomous Region (2022D01C766), Funding for graduate research and innovation projects in Xinjiang Uygur Autonomous Region (XJ2023G157).

Author contributions

Conceptualization and Supervision, ZX; Investigation, AS; Visualization, PA, YW; Resources, HL and MLL; Writing original draft, XZ; Reviewing, Editing, and Funding Acquisition, GY.

Data availability

All data in this study are true and reliable. The data that support the findings of this study are available from the corresponding author upon reasonable request. The remaining figure data are uploaded as Supplementary information.

Competing interests

The authors declare no competing interests.

References

1. Kachanova O, Lobov A, Malashicheva A (2022) The role of the Notch signaling pathway in recovery of cardiac function after myocardial infarction. Int J Mol Sci 23(20).
2. Kurian GA, et al. (2016) The role of oxidative stress in myocardial ischemia and reperfusion injury and remodeling: revisited.

Oxid Med Cell Longev 2016: 1656450.
3. Saki N, et al. (2022) Prevalence of cardiovascular diseases and associated factors among adults from southwest Iran: baseline data from Hoveyzeh cohort study. BMC Cardiovasc Disord 22(1): 309.
4. Binder P, et al. (2022) Pak2 regulation of Nrf2 serves as a novel signaling nexus linking ER stress response and oxidative stress in the heart. Front Cardiovasc Med 9: 851419.
5. Aarts P, et al. (2023) Validity and reliability of two digital wound measurement tools after surgery in patients with hidradenitis suppurativa. Dermatology 239(1): 99-108.
6. Liu C, et al. (2023) Comprehensive analysis of cuproptosis-related lncRNAs in immune infiltration and prognosis in hepatocellular carcinoma. BMC Bioinformatics 24(1): 4.
7. Liu Y, et al. (2022) Knockdown of long noncoding RNA LINC00240 inhibits esophageal cancer progression by regulating miR-26a-5p. Contrast Media Mol Imaging 2022: 1071627.
8. Mattick JS, et al. (2023) Long non-coding RNAs: definitions, functions, challenges and recommendations. Nat Rev Mol Cell Biol 24(6): 430-447.
9. Kopp F, Mendell JT (2018) Functional classification and experimental dissection of long noncoding RNAs. Cell 172(3): 393-407.
10. Ma L, Bajic VB, Zhang Z (2013) On the classification of long non-coding RNAs. RNA Biol 10(6): 925-33.
11. Chang H, Yao Y (2022) lncRNA TMPO antisense RNA 1 promotes the malignancy of cholangiocarcinoma cells by regulating let-7g-5p/high-mobility group A1 axis. Bioengineered 13(2): 2889-2901.
12. Lu P, et al. (2022) Noncoding RNAs in cardiac hypertrophy and heart failure. Cells 11(5).
13. Yu J, et al. (2020) Long noncoding RNA Ahit protects against cardiac hypertrophy through SUZ12 (suppressor of zeste 12 protein homolog)-mediated downregulation of MEF2A (myocyte enhancer factor 2A). Circ Heart Fail 13(1): e006525.
14. Foglia MJ, Poss KD (2016) Building and re-building the heart by cardiomyocyte proliferation. Development 143(5): 729-40.
15. Zhao MT, et al. (2020) Cardiomyocyte proliferation and maturation: two sides of the same coin for heart regeneration. Front Cell Dev Biol 8: 594226.
16. Yester JW, Kühn B (2017) Mechanisms of cardiomyocyte proliferation and differentiation in development and regeneration. Curr Cardiol Rep 19(2): 13.
17. Bishop SP, et al. (2021) Changes in cardiomyocyte cell cycle and hypertrophic growth during fetal to adult in mammals. J Am Heart Assoc 10(2): e017839.
18. Liu ZP, Olson EN (2002) Suppression of proliferation and cardiomyocyte hypertrophy by CHAMP, a cardiac-specific RNA helicase. Proc Natl Acad Sci U S A 99(4): 2043-8.
19. Lorenzen JM, Thum T (2016) Long noncoding RNAs in kidney and cardiovascular diseases. Nat Rev Nephrol 12(6): 360-73.
20. Zhang Y, et al. (2019) Long noncoding RNA MEG3 inhibits breast cancer growth via upregulating endoplasmic reticulum stress and activating NF-κB and p53. J Cell Biochem 120(4): 6789-6797.
21. Wan P, Su W, Zhuo Y (2017) The role of long noncoding RNAs in neurodegenerative diseases. Mol Neurobiol 54(3): 2012-2021.
22. Huang PS, et al. (2020) Dysregulated FAM215A stimulates LAMP2 expression to confer drug-resistant and malignant in human liver cancer. Cells 9(4).
23. Tripathi V, et al. (2010) The nuclear-retained noncoding RNA MALAT1 regulates alternative splicing by modulating SR splicing factor phosphorylation. Mol Cell 39(6): 925-38.
24. Sussman MA (2009) Mitochondrial integrity: preservation through Akt/Pim-1 kinase signaling in the cardiomyocyte. Expert Rev Cardiovasc Ther 7(8): 929-38.
25. Zeng N, et al. (2021) Diverging targets mediate the pathological role of miR-199a-5p and miR-199a-3p by promoting cardiac hypertrophy and fibrosis. Mol Ther Nucleic Acids 26: 1035-1050.
26. Boon RA, et al. (2016) Long noncoding RNAs: from clinical genetics to therapeutic targets? J Am Coll Cardiol 67(10): 1214-1226.